

## SYNTHESIS, CHARACTERIZATION AND REDOX BEHAVIOUR OF MIXED LIGAND COPPER(II) SACCHARINATE COMPLEXES

Grettel Valle-Bourrouet <sup>1\*</sup>, Larry R. Falvello<sup>2</sup> and Julio Gómez<sup>3</sup>

<sup>1</sup>School of Chemistry, University of Costa Rica, 11501-2060 San Jose, Costa Rica.

<sup>2</sup>Department of Inorganic Chemistry and I.C.M.A., University of Zaragoza-CSIC, Plaza San Francisco s/n, E-50009, Zaragoza, Spain.

<sup>3</sup>Department of Chemistry, University of La Rioja, Complejo Científico Tecnológico, Calle Madre de Dios 51, 26006 Logroño, Spain.

*Recibido 21 de julio, 2011; aceptado 31 de agosto, 2011*

### Abstract

Three mixed-ligand complexes of Cu(II) with saccharin (sac), pyrazole, (Hpz), imidazole, (Himid) were synthesized and characterized on the basis of elemental analysis, FT-IR spectroscopy, magnetic susceptibility, EPR spectra, and X-ray diffraction. The reaction of  $[\text{Cu}(\text{sac})_2(\text{H}_2\text{O})_4] \cdot 2\text{H}_2\text{O}$  with pyrazol in methanol resulted in a mononuclear pentacoordinated compound  $[\text{Cu}(\text{sac})_2(\text{Hpz})_3]$  (**1**) and a trinuclear N,N-bridged compound  $[\text{Cu}_3(\text{sac})_2(\text{Hpz})_3(\text{pz})_3]_2(\text{OH})$  (**2**), forming a nine membered  $[-\text{Cu}-\text{N}-\text{N}-]_3$  ring and  $\mu_3$ -OH bridge; each Cu(II) ion is tetracoordinated, with weak axial interactions from saccharinate ions. The Imidazole compound  $[\text{Cu}_2(\text{sac})_4(\text{Himid})_4]$  (**3**) has a dinuclear structure with two saccharinate ions as bridge; each Cu(II) ions has a penta-coordination sphere, two N-coordinated and one O-coordinated saccharinate ions on the equatorial plane, and two imidazole molecules in the axial positions.

### Resumen

Se sintetizaron tres complejos de cobre(II) con una mezcla de ligandos, sacarina (sac) y pirazol (Hpz) e imidazole (Himid). Los complejos se caracterizaron por análisis elemental, espectroscopía IR-FT, susceptibilidad magnética, esoelectroscopia EPR y difracción de rayos X. La reacción de  $[\text{Cu}(\text{sac})_2(\text{H}_2\text{O})_4] \cdot 2\text{H}_2\text{O}$  con pirazol en methanol produce un compuesto mononuclear pentacoordinado,  $[\text{Cu}(\text{sac})_2(\text{Hpz})_3]$  (**1**) y uno trinuclear  $[\text{Cu}_3(\text{sac})_2(\text{Hpz})_3(\text{pz})_3]_2(\text{OH})$  (**2**), con puentes N,N, que forman un anillo de nueve miembros  $[-\text{Cu}-\text{N}-\text{N}-]_3$  y un puente  $\mu_3$ -OH; cada átomo de cobre está tetracoordinado con una leve interacción axial de los iones sacarinato. El compuesto con imidazol  $[\text{Cu}_2(\text{sac})_4(\text{Himid})_4]$  (**3**) posee una estructura dinuclear con dos iones sacarinato puente, cada átomo de cobre está pentacoordinado, con dos

---

\* Corresponding author: grettel.valle@ucr.ac.cr

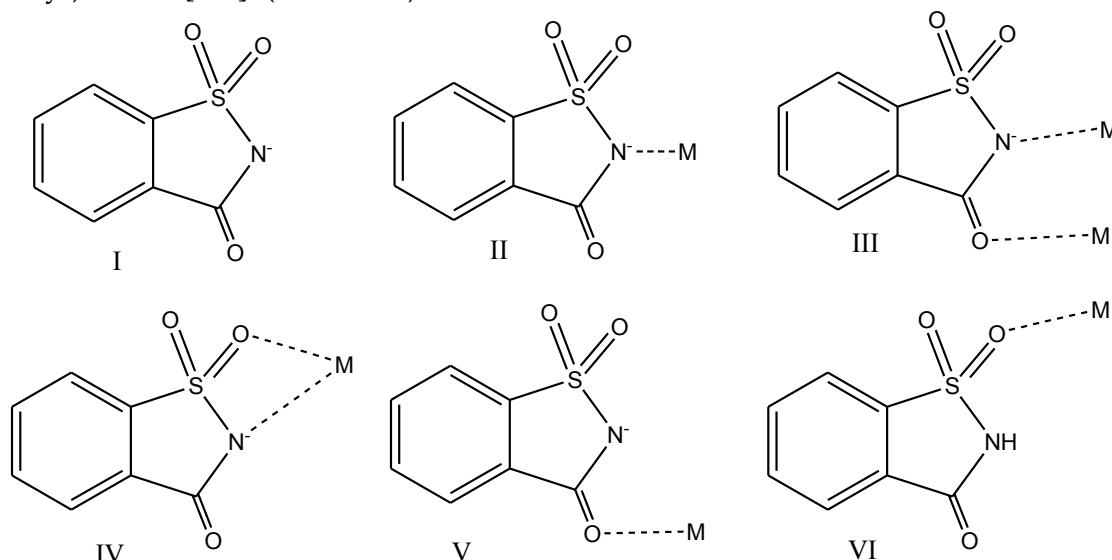
iones sacarinatos unidos por el átomo de nitrógeno y uno unido por un átomo de oxígeno en el plano equatorial y dos moléculas de imidazol en la posición axial.

**Keywords:** Saccharinate complexes, hydrogen bonds, pyrazole, imidazole, metal complexes, copper.

**Palabras clave:** complejo sacarinato, enlaces de hidrógeno, pirazol, imidazole, complejo metálico, cobre.

## I INTRODUCTION

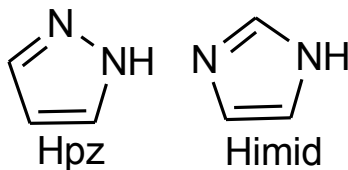
The saccharinate ion has been shown to be a very versatile ligand, since it offers different donor atoms to metal centers, namely N, O(carbonyl) and two O (sulfonyl) atoms. In certain cases it acts as a bridging or chelating ligand, through its N and O (carbonyl) atoms [1-5], (Scheme 1).



**Scheme I:** Saccharinate coordinations modes.

In the last years, there has been reported on mixed ligand complexes containing simultaneously saccharinate and some other ligands in the coordination sphere: pyridine [6,7], imidazole [5], 2,2'bipyridine [8]. These ligands can produce a change in the coordination mode of the saccharinate ligand. In the complex  $[V(\text{sac})_2(\text{py})_4]$  [6] it is coordinate through an O (carbonyl) atom, with imidazole acting as bridging ligand [5]. With this in mind we have attempted to prepare similar mixed-ligand complexes replacing imidazole by pyrazole, a five atoms ring molecule like imidazole, to carry out the reaction. Furthermore, pyrazole is an interesting ligand able to provide a 1,2-bridging form building multinuclear complexes[9]. The reaction, performed in water,

produced complexes of formula  $[M(\text{sac})_2(\text{Hpz})_2(\text{H}_2\text{O})_2]$ , where two water molecules were substituted by pyrazole molecules [10] and also  $[\text{Cu}(\text{sac})_2(\text{Hpz})_4]$ , where the saccharinate was bound to metal through the carbonyl oxygen atom [11].



Scheme II

Here we report the products of the reaction of copper saccharinate and pyrazole and, imidazole (scheme II) in methanol, to see if there are changes in the coordinations sphere of the saccharinate complexes. We describe here the crystal structures, spectroscopic, magnetic and electrochemical properties of the obtained products.

## II EXPERIMENTAL

**Methods and Materials:** Solvents, pyrazole, imidazole, copper nitrate, and sodium saccharinate were used as commercially available products. The complex  $[\text{Cu}(\text{sac})_2(\text{H}_2\text{O})_4] \cdot 2\text{H}_2\text{O}$ , was prepared as described in literature [12] and isolated as crystalline material.

**Physico-chemical measurements:** FT-IR spectra were recorded using KBr pellets with a Perkin Elmer Spectrum 100. Cyclic voltammperograms were performed with a computer controlled Autolab PGSTAT 10, in a nitrogen-saturated DMSO solutions with tetrabutylammonium hexafluorophosphate ( $\text{TBAPF}_6$ , 0.1 mol/L) as a supporting electrolyte, glassy carbon electrode as working electrode, platinum wire as counter electrode and  $\text{Ag}/\text{AgCl}$  as reference electrode.

X-band EPR spectra were recorded on a Bruker ESP 300 spectrometer. Simulation of EPR spectra were carried out using ESIM program. [13a]

Magnetic susceptibility data were measured from powder samples of solid material in the temperature range of 2-300 K by using a SQUIT susceptometer MPMS-7, Quantum Design with a field of 1.0T. The experimental data were corrected for underlying diamagnetism by the use of tabulated Pascal's constants. Simulation of magnetic susceptibility data were carried out using the JulX program (version 13). [13b] Intermolecular interactions were considered by using a Weiss temperature,  $\Theta_w$ , as a perturbation of the temperature scale,  $kT' = k(T - \Theta_w)$  for the calculation.

*X-Ray Crystallographic Data Collection and Refinement of the Structure***[Cu(C<sub>7</sub>H<sub>4</sub>NO<sub>3</sub>S)<sub>2</sub>(Hpz)<sub>3</sub>](1)**

A regularly shaped blue crystal was fixed to the end of a quartz fiber with epoxy. Geometric and intensity data were measured using a CAD-4 diffractometer. Data were reduced using the program XCAD4B [25]. Absorption corrections were based on eleven full or partial  $\psi$ -scans of reflections with Eulerian equivalent angle  $\chi$  in the range (-36.0) – (+62.0)°, thus achieving as broad as possible a dispersion of incident and diffracted beam directions [26]. The structure was solved by direct methods and refined by full-matrix least-squares. Hydrogen atoms were placed at calculated positions and treated as riding atoms in the refinement, with isotropic displacement parameters set to 1.2 times the equivalent isotropic displacement parameters of their respective parent atoms. The refinement converged with the residuals given in Table 1. The polar axis direction was established by refinement of the absolute structure parameter [27], which refined stably to a value of 0.00 (10).

**[Cu<sub>3</sub>(sac)<sub>2</sub>(Hpz)<sub>3</sub>(pz)<sub>3</sub>(OH)]·0.5(H<sub>2</sub>O)(2)**

A blue block-like crystal was mounted at the end of a quartz fiber using epoxy. Data were collected using routine procedures on a KappaCCD four-circle diffractometer [28]. Automated structure solution was carried out using the MAXUS software package [29]. The final development and refinement of the structure was done using SHELXTL [26]. Two partially occupied water sites, slightly more than 1 Å apart, were located and refined anisotropically with a common set of anisotropic displacement parameters for both, and with one-fourth occupancy each. Their hydrogen atoms were not located. The hydroxy hydrogen atom at the center of the cluster was located in a difference map and refined as a riding atom with its isotropic displacement parameter constrained to 1.2 times the equivalent isotropic displacement parameter of the carrier O atom. All of the remaining H atoms were placed at calculated positions and refined as riders with their U(iso) constrained to 1.2 U(eq) of their parent atoms. Final residuals are given in Table 1.

**Synthesis****[Cu(C<sub>7</sub>H<sub>4</sub>NO<sub>3</sub>S)<sub>2</sub>(Hpz)<sub>3</sub>](1) and [Cu<sub>3</sub>(sac)<sub>2</sub>(Hpz)<sub>3</sub>(pz)<sub>3</sub>(OH)]·0.5(H<sub>2</sub>O)(2)**

[Cu(sac)<sub>2</sub>(H<sub>2</sub>O)<sub>4</sub>]·2 H<sub>2</sub>O 0.50 g (1mmol) and pyrazole 0.30 g (4.4 mmol) were mixed in 50 mL methanol. The suspension was heated for 1h, and formed a deep blue solution. The solution, after standing overnight, yielded 0.3 g of bright blue prismatic crystals and 0.01g dark blue rectangular crystals. Both crystals obtained in this way were suitable for

X-ray analysis. Anal: Found for **1**: C 43.66, H 3.10, N 17.75 S10.32. Calc. For  $\text{CuC}_{22}\text{H}_{18}\text{N}_6\text{O}_7\text{S}_2$ : C43.65, H 3.19, N 17.71, S 10.0 14. Anal: Found for **2**: C 38.84, H 3.11, N 19.90. Calc. For  $\text{Cu}_3\text{C}_{32}$ ,  $\text{H}_{31}\text{N}_{14}$   $\text{O}_8$   $\text{S}_2$ : C 38.61, H 3.11, N 19.70.  $\lambda_{\text{max}}(\epsilon \text{mol}^{-1} \text{cm}^{-1})$ : 645(81),  $\mu_{\text{eff}}(\text{for } \mathbf{1})=1.90 \mu_{\text{B}}$ ,  $\mu_{\text{eff}}(\text{for } \mathbf{2})=1.92 \mu_{\text{B}}$ ,  $J= -211 \text{ cm}^{-1}$ ,  $g = 2.05$

### **[Cu<sub>2</sub>(C<sub>7</sub>H<sub>4</sub>NO<sub>3</sub>S)<sub>4</sub>(imid)<sub>4</sub>](3)**

[Cu(sac)<sub>2</sub>(H<sub>2</sub>O)<sub>4</sub>].2 H<sub>2</sub>O 0.53 g (1mmol) and imidazole 0.30 g (4.4 mmol) were mixed in 30 mL ethanol. The suspension was heated for 1h, and formed a sky blue solution after a few minutes, yielding 0.25 g (50%), of a brilliant sky blue precipitated. Suitable crystals for X were obtained from a slow evaporation of a dmf solution. Anal: Found: C 43.66, H 3.10, N 17.75 S10.32. Calc. For  $\text{CuC}_{22}\text{H}_{18}\text{N}_6\text{O}_7\text{S}_2$ : C43.65, H 3.19, N 17.71, S10. 14.  $\lambda_{\text{max}}(\epsilon \text{mol}^{-1}\text{cm}^{-1})$ : 699(90),  $\mu_{\text{eff}}$ . 2,63  $\mu_{\text{B}}$ .,  $J= -2.24 \text{ cm}^{-1}$ ,  $g = 2.15$ .

## III RESULTS AND DISCUSSION

*Description of the Crystal Structures.* Thermal ellipsoid drawings of the two structures, indicating the atom numbering schemes, are depicted in figures 1 and 2. Bond lengths and angles are given in table 2. The structure of **1** consists of a mononuclear compound, with a non-common (in the case of cooper saccharinate), pseudotrigonal bipyramidal coordination geometry around the central ion  $\text{Cu}^{2+}$ . Axial positions are occupied by two nitrogen atoms of pyrazole molecules. The carbonyl group's oxygen atom of one saccharinate ion, the nitrogen atom of the other saccharinate ion and a nitrogen atom of the pyrazole molecule build the trigonal plane. The orientation of each of the pyrazole rings was established on the basis of hydrogen bonds formed by the respective N-H moiety; these contacts are all too short to be C-H...A interactions, N(1)-N(4) 2.966 Å, O(5). There are some examples of O-bonded saccharinate ions, [V(sac)<sub>2</sub>(py)<sub>4</sub>].2py [6a], [Ni(sac)<sub>2</sub>(py)<sub>4</sub>].2py [6b], [Cr(sac)<sub>2</sub>(py)<sub>3</sub>] [6c], [Cu(dipyr)(N-sac)(O-sac)] and [Cu(sac)<sub>2</sub>(Hpz)<sub>4</sub>]. [11]. In all these cases the ion adopts this coordination position in spite of the normally preferred N-bonded, because of the steric hindrance caused by other molecules around the metal ion.

It can be seen in the significant different bond distances and angles in the plane of the molecule Cu-Osac 2.115(9) Å, Cu-Nsac 2.024(8) Å and Cu-Npz 1.986(9) Å., O1-Cu-N3 120.4°, Ni-Cu-N3 140.4° and N2-Cu-O1 99.2° The Cu-Osac distance in [Cu(dipyr)(N-sac)(O-sac)] is shorter 1.968(1) Å than **1**, while Cu-Nsac is practically the same 2.017(1) Å, in this case the molecule have a distorted square pyramidal geometry, with the two saccharinate ions in the plane of the pyramid.

Structure **2** consist of a trinuclear compound, a nine-membered [Cu-N-N]<sub>3</sub> metallcycle where each Cu atom is also coordinated to a pyrazole molecule. The center of this cycle accommodates triply bridging hydroxy molecule; the three Cu---O bonds

lengths are very similar, Table 2. Bond angles are 116.65 (8), 114.64 (8) and 117.27(8). The molecule ring's Cu-O distances and Cu-O-Cu angles are nearly similar to rings reported in the literature for the core  $[\text{Cu}_3(\mu_3\text{-OH})(\mu\text{-pz})_3]$  and for the core  $[\text{Cu}_3(\mu_3\text{-O})(\mu\text{-pz})_3]$  [14, 15a]. The Cu(1) atom is in a distorted square pyramidal geometry, intersecting in the apex position with the saccharinate ion, bound to the saccharinate ion nitrogen atom, N(13) with a distance of 2.343(2) Å. The other two copper ions have a weak interaction with the oxygen atoms from the  $\text{SO}_2$ -group, Cu(2)-O(3) 2.4981(18) Å and Cu(3)-O(4) 2.5468(18) Å. A second saccharinate molecule lies in the other side of the ring plane and interacts with the copper ions, Cu(2) and Cu(3) weaker than the first one, through one sulphonyl oxygen atom, Cu(3)-O(7), 2.8307(19) Å and the carbonyl oxygen, Cu(2)-O(5), 2.7079(18) Å. These two interactions build a very elongated pseudo-octahedral environment around the copper ions. The compound **2** is one of the rare examples of symmetric structure core  $[\text{Cu}_3(\mu_3\text{-OH})(\mu\text{-pz})_3\text{Hpz}_3]$  [14]. Other complexes with the core  $[\text{Cu}_3(\mu\text{-OH})(\mu\text{-pz})_3]$  are known [15], such as the series  $[\text{Cu}_3(\mu_3\text{-OH})(\mu\text{-pz})_3\text{Cl}_3]$ ,  $[\text{Cu}_3(\mu_3\text{-O})(\mu\text{-pz})_3\text{Cl}_3]$ ,  $[\text{Cu}_3(\mu\text{-Cl})_2(\mu\text{-pz})_3\text{Cl}_3]$  [15a], and the non symmetric structure core of  $[\text{Cu}_3(\mu_3\text{-OH})(\mu\text{-pz})_3(\text{Hpz})_2(\text{NO}_3)_2]$  [15c]. The structure of compound **3** was identical to the published by Liu et. al. [5]

The Cu-Nsac distance is comparable with the corresponding value in similar compounds, Cu (sac)<sub>2</sub>(py)<sub>2</sub>(H<sub>2</sub>O) 2.032(2) Å [16], Cu (sac)<sub>2</sub>(nic)<sub>2</sub>(H<sub>2</sub>O) (nic = nicotinic acid) 2.044(7) and 1.986(6) Å [11] and Cu (sac)<sub>2</sub>(4-propylpy)<sub>2</sub>(H<sub>2</sub>O) 2,021(4) c [17] and shorter than one found in Cu(sac)<sub>2</sub>(H<sub>2</sub>O)<sub>4</sub>·2H<sub>2</sub>O 2.061(2) [1]. The thiazole molecule is almost perpendicular to the plane of the saccharinato ligand. The angle between the corresponding best planes is 88.4°. The compound is further stabilized by relatively strong intermolecular hydrogen bonds. The water molecule is hydrogen bonded to two saccharinato carbonyl oxygen atoms forming an infinite chain of hydrogen bonds along the z axis. The O(16)···O(17) distance is 2.671(8) Å.

The C-O bonds in the three molecules lie around the average C-O distance 1.231 Å found for many saccharinate complexes [18].

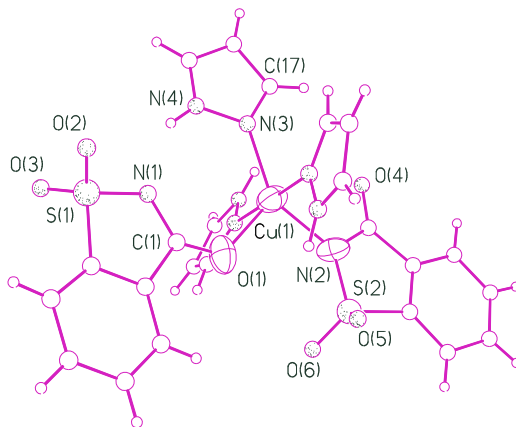


**Figure 1:** Drawing of the compound 1 showing 50% probability displacement ellipsoids

**Table 1:** Crystal data and structure refinement for  $\text{Cu}(\text{sac})_2(\text{Hpz})_3$  and  $[\text{Cu}_3(\text{sac})_2(\text{Hpz})_3(\text{pz})_3]_2(\text{OH})$

Empirical formula	$\text{C}_{23}\text{H}_{20}\text{CuN}_8\text{O}_6\text{S}_2$	$\text{C}_{32}\text{H}_{31}\text{Cu}_3\text{N}_{14}\text{O}_8\text{S}_2$
Formula weight	632,13	994.45
Temperature	298(2) K	123(2) K
Wavelength	0,71073 Å	0,71070 Å
Crystal system	Ortorrombic	Monoclinic
Space group	$\text{Pn } a 2(1)$	$\text{P}2_1/\text{n}$
Unit cell dimensions	$a = 14,3522(9) \text{ \AA}$ $\alpha = 90^\circ$ $b = 13,7018(11) \text{ \AA}$ $\beta = 90^\circ$ $c = 13,4286(18) \text{ \AA}$ $\gamma = 90^\circ$	$a = 17.8900(3) \text{ \AA}$ $\alpha = 90^\circ$ $b = 10.4590(2) \text{ \AA}$ $\beta = 94.2360(7)^\circ$ $c = 21.9190(5) \text{ \AA}$ $\gamma = 90^\circ$
Volume	$2640(4) \text{ \AA}^3$	$4090.09(14)$
Z	4	4
Density (calculated)	$1,590 \text{ Mg/m}^3$	$1.602 \text{ Mg/m}^3$
Absorption coefficient	$1,041 \text{ mm}^{-1}$	$1.712 \text{ mm}^{-1}$
F(000)	1292	2000
Crystal size	$0,21 \times 0,18 \times 0,16 \text{ mm}^3$	$0.28 \times 0.25 \times 0.25 \text{ mm}^3$
Theta range for data collection	$2,05 \text{ a } 24,95^\circ$	$1.42 \text{ to } 27,90^\circ$
Reflections collected	2420	26411
Independent reflections	2420 [R(int) = 0,0000]	9714 [R(int) = 0.0388]
Absorption correction	Psi-scans	multi-scan
Max. and min. transmission	0,8511 y 0,8110	0.959, 1.036
Refinement method	Full-matrix least.squares on $F^2$	Full-matrix least.squares on $F^2$
Data / restraints / parameters	2420/ 1/ 361	9714/ 0 / 535
Final R indices [I>2sigma(I)]	$R1 = 0,0630$ , $wR2 = 0,1137$	$R1 = 0.0379$ , $wR2 = 0.0808$
R indices (all data)	$R1 = 0,1330$ , $wR2 = 0,1392$	$R1 = 0.0592$ and $wR2 = 0.0860$
Largest dic. peak and hole	$0,296 \text{ y } -0,419 \text{ e.\AA}^{-3}$	$0.431, -0.469 \text{ e.\AA}^{-3}$

**Table 2:** Selected bond lengths (Å) and angles (°) for  $Cu(sac)_2(Hpz)_3$ , and  $[Cu_3(sac)_2(Hpz)_3(pz)_3]_2(OH)$ . **$Cu(sac)_2(Hpz)_3$** 

Cu-N(3)	1.986(9)	S(1)-O(3)	1.453(11)	N(7)-Cu-N(2)	92.8(5)
Cu-N(7)	2,008(11)	S(2)-O(5)	1.455(8)	N(5)-Cu-N(2)	89.1(5)
Cu-N(5)	2,012(10)	S(2)-O(6)	1.430(9)	N(3)-Cu-O(1)	120.4(4)
Cu-N(2)	2,024(8)			N(7)-Cu-O(1)	87.3(4)
Cu-O(1)	2,115(9)	N(3)-Cu-N(7)	90,4(4)	N(5)-Cu-O(1)	90.0(4)
C(3)-O(12)	1,248(14)	N(3)-Cu-N(5)	89.6(4)	N(2)-Cu-O(1)	99.2(4)
C(8)-O4	1,217(12)	N(7)-Cu-N(5)	177.0 (5)	N(7)-Cu-N(2)	92.8(5)
S(1)-O(2)	1.447(11)	N(2)-Cu-N(3)	140.4(4)		

 **$[Cu_3(sac)_2(Hpz)_3(pz)_3]_2(OH)$** 

Cu(1)-N(6)	1.964(2)	Cu(3)-N(4)	1.949(2)	N(6)-Cu(1)-N(1)	166.57(9)
Cu(1)-N(1)	1.965(2)	Cu(3)-N(5)	1.953(2)	N(6)-Cu(1)-O(1)	87.60(8)
Cu(1)-N(22)	2,0216(11)	Cu(3)-O(1)	1.9853(16)	N(1)-Cu(1)-O(1)	87,85(8)
Cu(1)-N(7)	2,008(2)	Cu(3)-N(11)	2.012(2)	O(1)-Cu(1)-N(7)	164.62(8)
Cu(1)-O(1)	1.9943(16)	Cu(3)-O(4)	2.5468(18)	N(3)-Cu(2)-N(2)	173.09(9)
Cu(1)-N(13)	2.343(2)	Cu(3)-O(7)	2.8307(19)	O(1)-Cu(2)-N(9)	178.05(8)
Cu(2)-N(2)	1.971(2)	C(19)-O(2)	1.236(3)	N(3)-Cu(2)-O(1)	88.68(8)
Cu(2)-O(1)	1.9832(16)	C(26)-O(5)	1.237(3)	N(2)-Cu(2)-O(1)	88.34(8)
Cu(2)-N(9)	1.989(2)	S(1)-O(4)	1.4470(18)	N(11)-Cu(3)-O(1)	176.52(8)
Cu(2)-O(3)	2.4981(18)	S(2)-O(7)	1.4455(19)	N(4)-Cu(3)-N(5)	176.90(9)
Cu(2)-O(5)	2.7079(18)	S(2)-O(6)	1.4414(19)	O(1)-Cu(3)-N(4)	88.92(8)
				N(5)-Cu(3)-O(1)	88.04(8)
		Cu(3)-N(4)	1.949(2)	N(6)-Cu(1)-N(1)	166.57(9)
				Cu(1)-O(1)-Cu(2)	114.64(8)
				Cu(1)-O(1)-Cu(3)	117.27(8)
				Cu(2)-O(1)-Cu(3)	116.65(8)

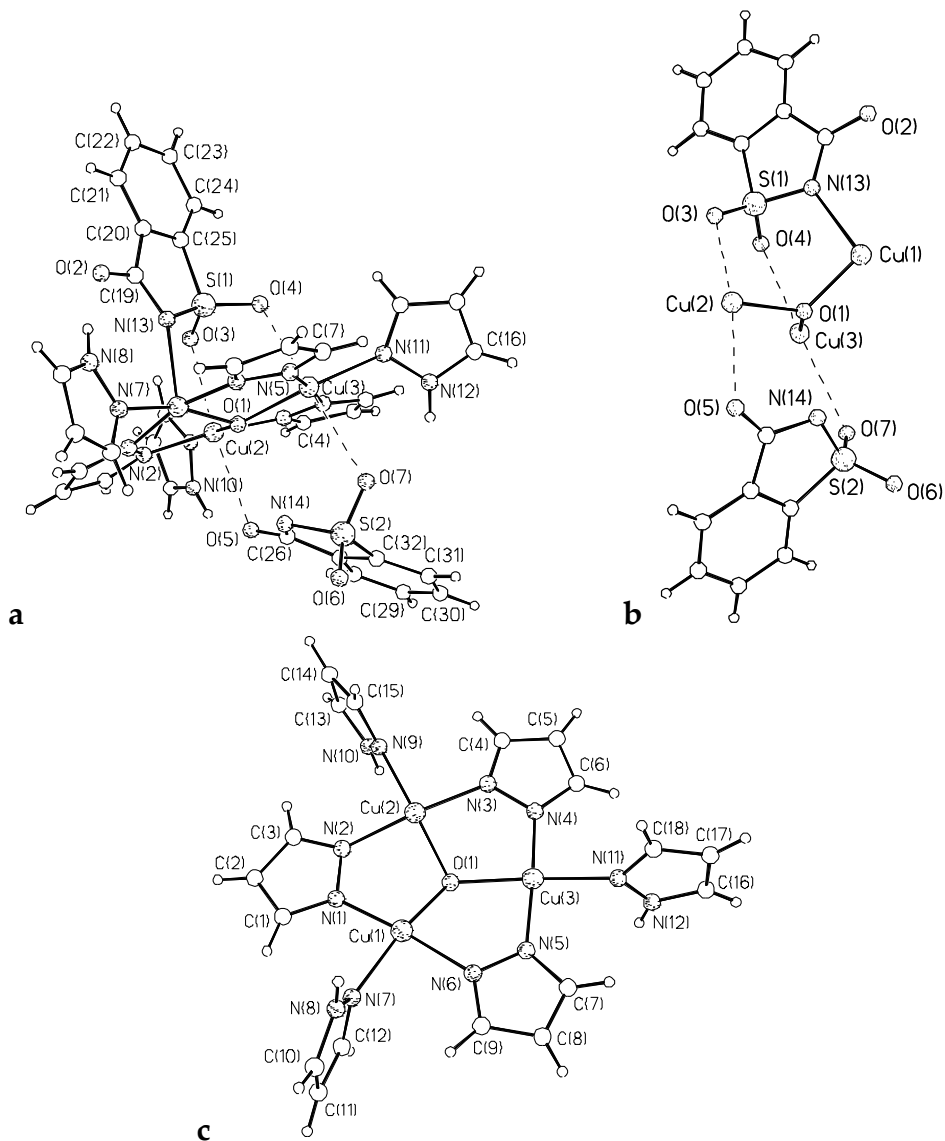


**Figure 2:** a. Drawing of the compound **2** showing 50% probability displacement, b, detail of the saccharinate interactions with the copper ions, c, and plane of the molecule, c.

### Spectroscopic properties

The principal IR bands and magnetic data are shown in table 4. The compounds of this work show different IR patterns, due to the different ligand coordination around the central ion. The compounds **1**, **2** and **3** show bands between  $3300\text{ cm}^{-1}$  and  $3100\text{ cm}^{-1}$  due to the pyrazole  $\nu(\text{N-H})$  bands. Free pyrazole molecule shows several strong N-H stretching bands between  $3300$  and  $2600\text{ cm}^{-1}$ .

The assignment of the  $\nu(\text{C=O})$  mode in the IR spectra of the four compounds was made by taking into account a number of previous assignments and calculations [16, 17, 18]. Complexes **1** and **3** show N- and O-coordinated saccharinate molecules, that is

reflected in the  $\nu(\text{C}=\text{O})$  frequency split of the respective carbonyl stretchings, amounting to  $26\text{ cm}^{-1}$ . In complex **2**, the  $\nu(\text{C}=\text{O})$  frequency,  $1632\text{ cm}^{-1}$ , is lower than the N-coordinate saccharinate in **1** probably due to the higher ionic character of the saccharinate ions that are weak N- bonded to copper ion, permitting a charge delocalization in the molecule with a reduction of the electron density and also the force constant of the C-O bond.

The spectroscopic data are consistent with penta-coordination geometry and indicate that the structure showed in solid state is preserved when in solution. The  $\lambda_{\text{max}}$  values are blue-shifted, respect to tetra-hydrated sacharinate complexes, as expected for pyrazole, a stronger ligand than water [20].

**Table 3:** Spectral and magnetic data for the compounds.

N°	Complex	Infrared spectra					Electronic spectra	
		$\nu(\text{O-H})$	$\nu(\text{N-H})$	$\nu(\text{C=O})$	$\nu_{\text{as}}(\text{S=O})$	$\nu_{\text{s}}(\text{S=O})$	$\lambda_{\text{max}}/\text{nm}$ $\epsilon/\text{mol}^{-1}\text{ cm}^{-1}$	$\mu_{\text{eff}}/\mu_{\text{B}}$ , $\text{J}/\text{cm}^{-1}, \text{g}$
1	$\text{Cu}(\text{sac})_2(\text{pz})_3$		3279/3136	1663/1637	1290	1154	645 (81)	1.90
2	$[\text{Cu}_3(\text{sac})_2(\text{Hpz})_3(\text{pz})_2(\text{OH})]$		3322	1630	1273	1148		-1.92, -2.24, 2.15
3	$\text{Cu}_2(\text{sac})_4(\text{imid})_4$		3366/3340	1673	1287	1156/1168	699(90)	2.60, -2.17, 2.14

### Magnetic properties

The effective magnetic moments at room temperature for **1**,  $1.90\ \mu_{\text{B}}$ , is in the range expected for mononuclear copper(II) complexes.

To investigate the magnetic behavior of the multinuclear copper complexes **2** and **3**, the magnetic susceptibility of these compounds was measured in the temperature range of 2-300 K.

The temperature dependence of  $\mu_{\text{eff}}$  for compound **2** is given in Figure 3. At room temperature  $\mu_{\text{eff}}$  is very low ( $1.92\ \mu_{\text{B}}$ ) with respect to the value expected for the three independent Cu(II) ions (around  $3\ \mu_{\text{B}}$ ). As the temperature is lowered  $\mu_{\text{eff}}$  decreases, reaching a value around  $1.73\ \mu_{\text{B}}$  at 70 – 50 K, which correspond to the spin-only value for one unpaired electron. This behavior indicates a moderate strong antiferromagnetic

interaction between the copper ions, with an unpaired electron per Cu<sub>3</sub> unit in the ground state; the  $\mu_{\text{eff}}$  value keeps on decreasing below the 50 K until 2K, reaching a value of 1.49  $\mu_{\text{B}}$ . as observed in similar compounds [15]. Considering that the three metals are structurally almost equivalent, it can be assumed that the exchange coupling constants are identical,  $J_1 = J_2 = J_3 = J$ , so the spin Hamiltonian  $H = -J(S_1S_2 + S_2S_3 + S_1S_3)$  will describe the interactions of the spins. From this Hamiltonian, a solution of magnet susceptibility may be derived as follows:

$\chi_{\text{M}} = (N\beta^2g^2/4kT)[1 + 5\exp(3J/2kT)]/[1 + \exp(3J/2kT)]$ , where  $N$ ,  $g$ ,  $\beta$ ,  $k$  and  $T$  have their usual meanings.

Due to the low temperature behavior, the Weiss correction parameter  $\Theta$  was included, for possible intertrimer magnetic interaction ( $T$  replaced by  $T-\Theta$ ). The simulation of the susceptibility data using the above Hamiltonian, fit to  $J = -212 \text{ cm}^{-1}$  with  $g = g_1 = g_2 = g_3 = 2.06$ , a temperature independent paramagnetism (TIP) of  $200 \cdot 10^{-6} \text{ cm}^3 \text{ mol}^{-1}$  and a Weiss temperature of  $-3 \text{ K}$ . Attempts at getting a better fit by using an equation with two different  $J$  values (so treating the system as an isosceles triangle) were also performed. The  $J$  and  $J'$  values obtained, very similar, did not significantly differ from those obtained with only one  $J$  value, and the goodness of the fitting did not improve.

The obtained  $J$  value is consistent with reported values for analogous compounds that are around  $200 \text{ cm}^{-1}$  [15].

The temperature variation of the effective magnetic moment of **3** is show in Figure 4. The value of  $\mu_{\text{eff}}$  2.60  $\mu_{\text{B}}$  decreases with decreasing temperature to 2.49  $\mu_{\text{B}}$  at 20 K and 1.06  $\mu_{\text{B}}$  at 2 K. This behavior is consistent with very weak antiferromagnetic interaction between the copper(II) ions. The data were fitting using the Hamiltonian  $H = -2JS_1S_2$ , the obtained best fit parameters are:  $J = -2.17 \text{ cm}^{-1}$ ,  $g = 2.14$ , a TIP of  $160 \text{ cm}^3 \text{ mol}^{-1}$ , a paramagnetic impurity, PI = 0.2 %. Similar magnetic data were obtained for  $[\text{Cu}_2(\text{C}_6\text{H}_3\text{Cl}_2\text{OCH}_2\text{COO})_4(\text{bipyam})_2]$ ,  $\text{C}_6\text{H}_3\text{Cl}_2\text{OCH}_2\text{COO} = 2,4$  dichlorophenoxyacetato,  $J = -0.8 \text{ cm}^{-1}$ ,  $g = 2.12$  [20] and for  $[\text{Cu}_2(2\text{-MeSnic})_2(\text{py})_2]_2$ ,  $J = -0.65 \text{ cm}^{-1}$ ,  $g = 2.12$ , 2-MeSnic = 2-methylthionicotinate. [22]. The values of  $2J$  for these compounds  $-4.34$ ,  $-1.60$  and  $-1.30$  suggest that the magnetic orbitals are unfavourably oriented to provide good overlap for a magnetic interaction. [23]

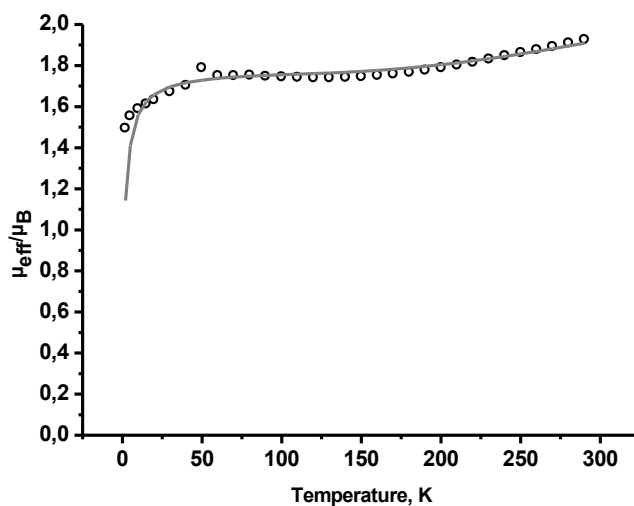


**Figure 3:** Plot of the magnetic moment of  $[\text{Cu}_3(\text{sac})_2(\text{Hpz})_3(\text{pz})_3]_2(\text{OH})$  as a function of temperature. The solid line represent the best fitting curve.

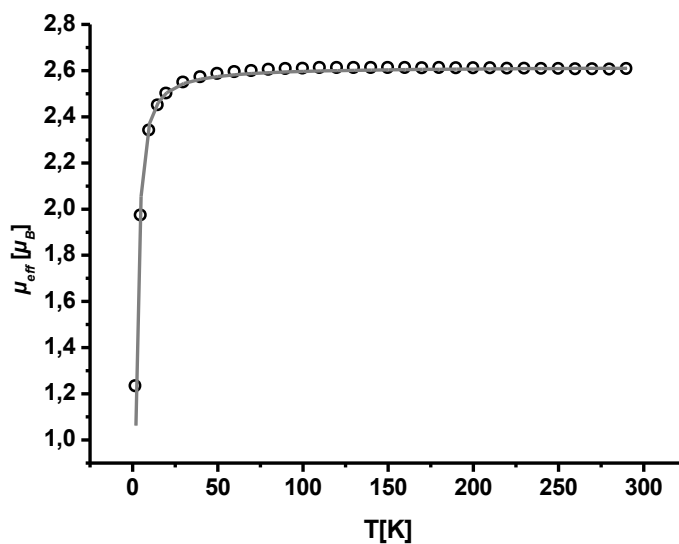


**Figure 4:** Plot of the magnetic moment of  $[\text{Cu}_2(\text{sac})_4(\text{Himid})_4]$  as a function of temperature. The solid line represent the best fitting curve.

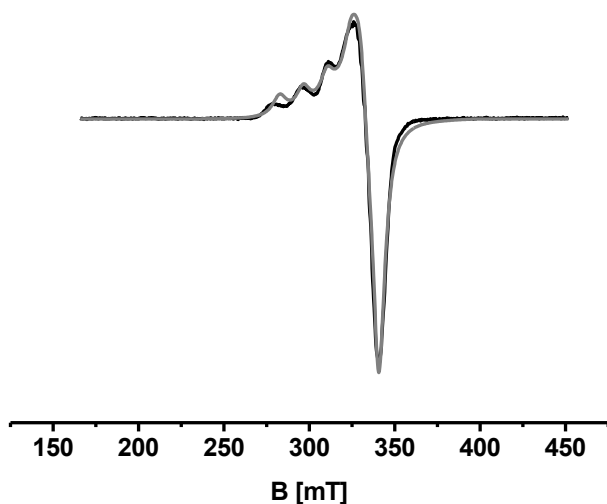


**Figure 5:** EPR spectrum of  $[\text{Cu}(\text{sac})_2(\text{pyr})_3]$  in dichloromethan solution, the gray line is the best simulations data.

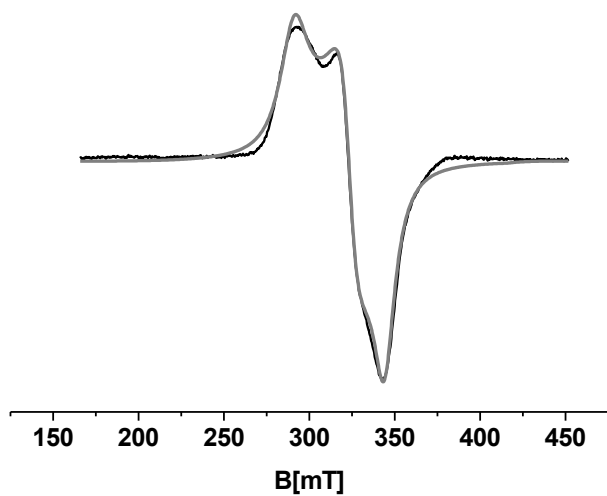


**Figure 6:** EPR spectrum of a polycrystalline sample  $[\text{Cu}(\text{sac})_2(\text{imid})_2]_2$  in dichloromethan solution, the gray line is the best simulation data.

### Electrochemistry behavior of the compounds

The redox properties of the complexes **1** and **3**, were determined by cyclic voltammetry measurements, carried out in dimethylformamide at room temperature with a scan rate of  $100 \text{ mVs}^{-1}$ . For compound **1** one quasi-reversible single-electron oxidation wave was observed (Figure 7), and an irreversible reduction peak for **1**, at  $-0.23 \text{ V}$ . The oxidation half-wave potentials were  $0.43$  and  $0.45 \text{ V}$  respectively.

Compound **3** showed a reversible one electron wave at 0.3 V.,  $I_o/I_R = 1$  and  $\Delta E = 0.14$  V, the last value should be 0.059, but due to the solution resistance that produce big wave peak separation, it was compared with the ferrocene, Fc/Fc<sup>+</sup>,  $\Delta E$  value (0.141 V) in the same solution, to confirm the wave reversibility. In table 4, pKa values for heterocyclic amine and the  $E_{1/2}$  are given. Imidazole is more basic amine and has the smallest  $E_{1/2}$  value, which means that more dative character can stabilize the high oxidation state.

**Table 4.** Electrochemical data of compounds **1**, **3** and **4** and pKa values for the corresponding ligands.

<b>Compound</b>	$E_{1/2}$ , V	$\Delta E$ , V	<b>Pka, amine</b>
<i>Cu(sac)<sub>2</sub>(pz)<sub>3</sub></i>	0,43 q,	0,18	2,48
<i>Cu<sub>2</sub>(sac)<sub>4</sub>(imid)<sub>4</sub></i>	0,31 r	0,14	6,99
Fc/Fc <sup>+</sup>	0,61	0,14	

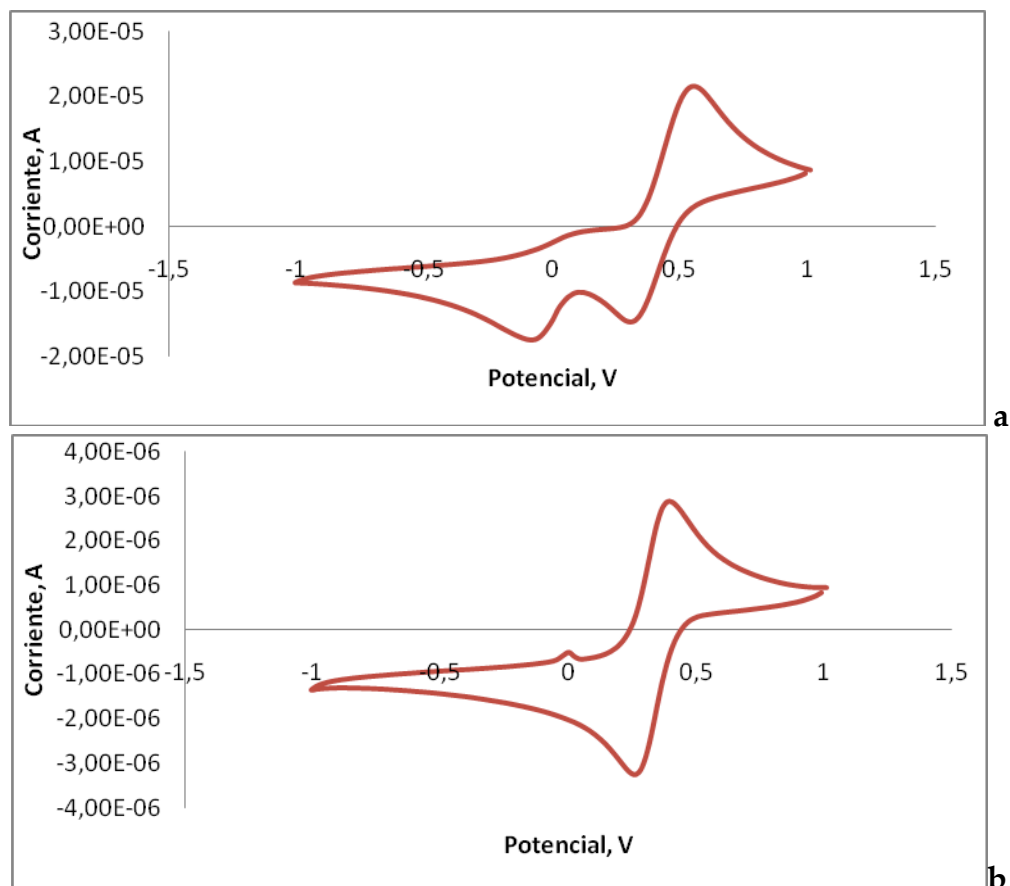


**Figure 7:** Cyclic voltammogram in DMF/TBAPF<sub>6</sub> 0.1 mol L<sup>-1</sup> on a glassy carbon electrode vs Ag/AgCl, of the copper complex a [Cu(sac)<sub>2</sub>(pyr)<sub>3</sub>], b. [Cu<sub>2</sub>(sac)<sub>4</sub>(imid)<sub>4</sub>].

#### IV CONCLUSIONS

The product of the reaction between copper saccharinate and pyrazole, depends on the reaction conditions. If the reaction is made in water solution the products are [Cu(sac)<sub>2</sub>(Hpz)<sub>2</sub>(H<sub>2</sub>O)<sub>2</sub>] [10] and [Cu(sac)<sub>2</sub>(Hpz)<sub>4</sub>] [11], the difference lies maybe in the water amount used for the reaction, because the mol ratios of Cu complex/ pyrazole were the same in both cases. The reaction in methanol produces also two compounds, in this case from the same reaction, [Cu(sac)<sub>2</sub>(Hpz)<sub>3</sub>] and [Cu<sub>3</sub>(sac)<sub>2</sub>(Hpz)<sub>3</sub>(pz)<sub>3</sub>]<sub>2</sub>(OH)]. The last compound is the result of the auto-deprotonation of pyrazole, pK<sub>a</sub> = 2.48. This compound was reproduced from the reaction in basic media. Imidazole gave the same compound independent of the reaction media, water, methanol or DMF. They have the same size, the basicity could be a reason, Imidazole pK<sub>a</sub> = 6.99 and pyrazole 2.48. [24].

## V REFERENCES

- [1] S. Z. Heider, K. M. A. Malik, K.J. Ahmed, H. Hess. H. Riffel, M. B. Hursthouse, *Inorg. Chim. Acta* **1983**, 72, 21.
- [2] F. A. Cotton, G.E. Lewis, C. A. Murillo, W. Schwotzer, G. Valle, *Inorg. Chem.* **1984**, 23, 4038.
- [3] G. Javanovski, B. Kamenar *Crysrt. Struct. Comm.* **1982**, 25, 3423.
- [4] ] F. A. Cotton, L.R. Falvello, , C. A. Murillo, W. Schwotzer, G. Valle-Bourrouet, *Inorg. Chim. Acta* **1991**, 190, 89.
- [5] S. Liu, J. Huang, J. Li, W. Lin *Acta Crystallogr.* **1991**, C47, 41.
- [6] a. F. A. Cotton, L.R. Falvello, R. Llusar, E. Libby, C. A. Murillo, W. Schwotzer, *Inorg. Chem.* **1986**, 25, 3423. b. Quinzani, O. V.; Tarulli, S.; Marcos, C. García Granda, S.; Baran, E. J. Z. *anorg. allg. Chem.* **1999**, 625, 1948. c. Alfaro, N. M.; Cotton, F. A.; Daniels, L. M.; Murillo, C. A. *Inorg. Chem.* **1992**, 2718.
- [7] G. Jovanovski, P. Naumov, O. Grupce, B. Kaitner, *Eur. J. Solid. State Inorg. Chem*, **1998**, 35, 231.
- [8] A. Hergold-Brundic, O. Gupce, G. Javanovski, *Acta Crystallogr.* **1991**, C47, 2659.
- [9] Sadimenko, A. P.; Basson, S.S. *Coord. Chem. Rev.* 1996, 147, 247.
- [10] L. W. Pineda-Cedeño, L. R. Falvello, R. Llusar , T. Weyhermueller, G. Valle-Bourrouet, *Polyhedron*.
- [11] Naumov, P.; Jovanovski, G.; Drew, M. G. B.; Ng S. W. *Inorg. Chim. Acta* **2001**, 314, 154.
- [12] ]Quinzani, O. V.; Tarulli, S.; Marcos, C. García Granda, S.; Baran, E. J. Z. *anorg. allg. Chem.* **1999**, 625, 1948.
- [12] S. Z. Haider, K.M.. Malik, K.J. Ahmed, *Inorg. Synth.*, **1985**, 23, 47.
- [13] a. Bill, E. Simulation of EPR spectra program ESIM, Max Planck Institut for Bioinorganic Chemistry, Mülheim an der Ruhr. b. Bill. E. Simulation of molecular

magnetic data, program julX (version 1.3), Max Planck Institut for Bioinorganic Chemistry, Mülheim an der Ruhr.

[14] **a.** Sakai, K.; Yamada, Y.; Tsubomura, T.; Yabuki, M.; Yamaguchi, M. *Inorg. Chem.* **1996**, *35*, 542. **b.** Shen, W. Z.; Yi, I.; Cheng, P.; Yan, S. P.; Liao, D. Z.; Jiang, Z. H. *Inorg. Chem. Comm.* **2004**, *7*, 819.

[15] **a.** Angaridis, P. A.; Baran, P.; Boča, R.; Cervantes–Lee, F.; Haase, W.; Mezei, G.; Raptis, R. G.; Werner, R. *Inorg. Chem.* **2002**, *41*, 2219. **b.** Boča, R.; Dlháň. L.; Mezei, G.; Ortiz-Perez T.; Raptis, R. G.; Telsler, J. *Inorg. Chem.* **2003**, *42*, 5801. **c.** Hulsbergen, F. B. ten Hoet, R. W. M.; Verschoor, G.C.; Reedijk, J. *J. Chem. Soc. Dalton Trans.* **1983**, 539. **d.** Colacio, E.; Dominguez-Vera, J. M.; Escuer, A.; Klinga, M.; Kivekäs, R.; Romerosa, A. *J. Chem. Soc. Dalton Trans.* **1995**, 343. **e.** Ferrer, S.; Haasnoot, J.G.; Reedijk, J.; Müller, E.; Bianini Cingi, M.; Lanfranchi, M.; Manotti Lanfredi, A. M.; Ribas, J. *Inorg. Chem.* **2000**, *39*, 1859.

[16] Jovanovski, G.; Naumov, P. Grupče, O.; Kaitner, B. *Eur. J. Solid State Inorg. Chem.* **1998**, *35*, 231.

[17] Naumov, P.; Jovanovski, G.; Ristova, M.; Razak, I. A.; Cakir, S., Chantrapromma, S.; Fun, H. K.; Ng, S. W. Z. *Anorg. Allg. Chem.* **2002**, *628*, 2930.

[18] Naumov, P.; Jovanovski, G. *Struct. Chem.* **2000**, *11*, 19.

[19] Lever A. B. P. *Inorganic Electronic Spectroscopy*, 2 ed. Elsevier: Amsterdam, 1984.

[20] **a.** Falk, M.; Huang, C. H.; Knop, O. *Can. J. Chem.* **1975**, *53*, 5. **b.** Falk, M.; Knop, O. *Can. J. Chem.* **1977**, *55*, 1736.

[21] Psomas, G.; Raptopoulou, C. P.; Iordanidis, L.; Dendrinou-Samara, C.; Tangoulis, V.; Kessissoglou, D. P. *Inorg. Chem.* **2000**, *39*, 3042.

[22] Segl'a, P.; Palicová, M.; Mikloš, D.; Koman, M.; Melník, M.; Korabik, M.; Mrozinski, J.; Glowiak, T.; Sundenber, M. R.; Lönnecke, P. *Z. Anorg. Allg. Chem.* **2004**, *630*, 470.

[23] Kahn, O. *Molecular Magnetism*, VCH Publishers, New York, 1993.

[24] Vaughan, J.D.; Fullerton, D. C.; Chang, C. A. *Intern. J. Quant. Chem.* **1968**, 205.

[25] Harms, K. & Wocadlo, S. (1996). XCAD4. University of Marburg, Germany.

[26] Except where indicated otherwise, crystallographic calculations, including absorption corrections, were performed with the commercial package SHELXTL. Bruker (2001). *SHELXTL*. Bruker AXS Inc., Madison, Wisconsin, USA.

[27] Flack, H. D. *Acta Cryst.* **1983**, **A39**, 876-881.

[28] Nonius (1999). *COLLECT*. Nonius BV, Delft, The Netherlands.

[29] Mackay, S., Gilmore, C. J., Edwards, C., Stewart, N. & Shankland, K. (1999). *MAXUS*. Nonius BV, Delft, The Netherlands, MacScience Co. Ltd, Japan, and University of Glasgow, Scotland.

### **Acknowledgements**

We are grateful to the Vicerrectoría de Investigación, University of Costa Rica; (Grant No. 115-98 375) for financial support. GVB thanks DAAD for a research fellowship and Prof. Karl Wieghardt for the use of research facilities at Max-Planck-Institute for Bioinorganic Chemistry. Funding was also provided by the Ministry of Science and Innovation (Spain) under Grant MAT2008-04350 and CONSOLIDER-INGENIO in Molecular Nanoscience, ref. CSD 2007-00010, and by the Diputación General de Aragón (Spain)

### **Appendix. Supplementary material**

Crystallographic data for the structures reported in this paper have been deposited with the Cambridge crystallographic Data Center as supplementary publication Nos 784928 (1) & 784929 (2). Copies of the data can be obtained free of charge on application to The Director, CCDC, 12 Union Road, Cambridge CB2 1EZ, UK, fax: int.code+(1223)336-033; e-mail for inquiry: fileserv@ccdc.cam.ac.uk.